Imbalanced speciation pulses sustain the radiation of mammals

Ignacio Quintero, Nicolas Lartillot, Hélène Morlon

Imbalanced speciation pulses sustain the radiation of mammals

Ignacio Quintero[1], Nicolas Lartillot[2], Hélène Morlon[1]

[1] Institut de Biologie de l'ENS (IBENS), Département de biologie, École normale supérieure, CNRS, INSERM, Université PSL, 75005 Paris, France

[2] Laboratoire de Biométrie et Biologie Évolutive UMR, CNRS, Université Lyon, Université Lyon 1, 69622 Villeurbanne, France

One Sentence Summary: Mammal diversity resulted from the evolutionary success of fast-speciating lineages that withstood the K-Pg mass extinction event.

Abstract

The evolutionary histories of major clades, including mammals, often comprise changes in their diversification dynamics, but how these changes occur remains debated. We combine comprehensive phylogenetic and fossil information in a new 'birth-death diffusion' model that provides a detailed characterization of variation in diversification rates in mammals. We found an early-rising and sustained diversification scenario, wherein speciation rates increased before and during the Cretaceous-Paleogene (K-Pg) boundary. The K-Pg mass extinction event filtered out more slowly speciating lineages, and was followed by a subsequent slowing in speciation rates rather than rebounds. These dynamics arose from an imbalanced speciation process, with separate lineages giving rise to many, less speciation-prone descendants. Diversity seems to have been brought about by these isolated, fast speciating lineages, rather than by a few punctuated innovations.

Main Text

Understanding the tempo and mode by which lineages diversify is fundamental to explaining variation of biodiversity across space, time and taxa (*1*). The remarkable diversity present across the tree of life generally results from episodes of fast lineage diversification that underlie successful evolutionary radiations (*2*). Special attention has been given to understanding the timing of such pulses with respect to major abiotic events and the mode in which these pulses occur in some lineages and not in others, with no general consensus. Throughout the over 200 My evolutionary history of mammals, for instance, environmental factors such as the radiation of flowering plants (i.e., the Cretaceous Terrestrial Revolution), the Cretaceous-Paleogene (K-Pg)

extinction event, the Paleocene-Eocene Thermal Maximum (PETM), and other major environmental events, likely spurred distribution shifts and extinctions, together with novel ecological opportunities, generating widespread diversification pulses (*3–6*). Most often discussed is the role of the K-Pg event, in particular, with hypotheses that posit that fast diversification occurred either before, at, or after the event, dubbed as 'early-', 'explosive-' or 'delayed-' rise of extant mammals, respectively (*3–5, 7–11*).

A long-standing paradigm holds that such shifts in the speed of diversification occur discretely and sporadically, driven by changes in the environment or the acquisition of adaptive evolutionary novelties, i.e., 'key innovations' (Fig. 1A) (*12–16*). Here, fast diversification is clade-wide, linked to the rapid filling of a niche space that has been freed from other occupants (e.g., due to environmentally-driven mass extinctions), or opened by a major evolutionary innovation. Since early observations that richness is highly unevenly distributed across the tree of life (*17*), much effort has been devoted to identifying the clade-wide increases in diversification rates that supposedly occurred at the origin of the most diverse species groups (*13, 18–20*). However, evidence of substantial intra-clade heterogeneity in diversification rates, beyond that expected from large clade-level dynamics, challenges this paradigm (*21–27*). An alternative view considers changes in diversification rates to be less predictable and more dynamic, giving prominence to the role of contingency in driving evolutionary outcomes (Fig. 1B) (*28, 29*). Here, the interplay between species' evolving ecologies and their particular spatial and environmental contexts could occasionally lead to short periods of fast diversification in specific lineages.

A fine-grained consideration of diversification

Here we develop the birth-death diffusion model (Fig. 1B, (*30*)), designed to provide a flexible framework that simultaneously enables the reconstruction of overarching diversification dynam-

ics and of fine-grained stochasticity of speciation and extinction rates. The process starts with a lineage with speciation rate λ_0 and extinction rate μ_0. Lineage-specific speciation ($\lambda_l(t)$) and extinction ($\mu_l(t)$) rates then evolve in time following a Geometric Brownian motion (Fig. 1B). Rates are inherited at speciation; this hypothesis of inheritance is implicit (and in fact stronger) in all phylogenetic and paleontological diversification models that assume rate homogeneity within specific time-bins or sub-clades, and is justified by the inheritance of traits that may modulate diversification rates. A drift term α reflects temporal trends in speciation and avoids the "run-away species selection" that the birth-death diffusion model and others with inherited speciation rates sometimes produce (*14,26,31*). Two diffusion terms, σ_λ and σ_μ, reflect variability in speciation and extinction rates, respectively. The model can be simplified by imposing constraints. For example, we can assume no extinction, constant extinction rate, or constant turnover (ratio of extinction to speciation rate). Finally, we can constrain the extinction rate to follow a specific trajectory, such as a curve (or subclade-specific curves) separately estimated from the fossil record.

Given a phylogeny of present-day species, we developed an approach to obtain "complete" trees under the birth-death diffusion model, that is, trees with all of the extinct and unsampled lineages, together with instantaneous lineage-specific diversification rate estimates ((*30*), fig. S1). Our approach relies on Bayesian data augmentation techniques, which provide a probabilistic model-based imputation. Contrary to other imputation methods, the augmented data that arises from this procedure does not influence the posterior parameters of the model given the observed data (*32*). This allows us to estimate paleodiversity curves, i.e., variations in species richness through time, as well as speciation rates averaged over both lineages that are observed in the empirical tree and lineages that are not. We account for potential missing species in the extant phylogeny using clade-specific sampling probabilities. We validated the approach using simulations (*30*) (figs. S2-S9). Importantly, while the Brownian diffusion assumption may lead

to smoothing of the reconstructed diversification trajectories, simulations under scenarios of cross-species variation in speciation rates along time or punctuated diversification rate shifts in specific lineages along the tree (i.e. the scenario depicted on Fig. 1A) show that the birth-death diffusion model is able to recover sudden variations (fig. S8-S9).

When constraining extinction rates to follow estimates from the fossil record, the birth-death diffusion model exploits the advantages of the complementary sources of evolutionary information provided by neontological and paleontological data. Time-calibrated phylogenetic trees built from genetic data contain topological information under a branching process, providing information on ancestral-descendant relationships across thousands of lineages, while fossil information provides direct evidence of past extinction dynamics, including mass extinction events (*33–35*).

Heterogeneity of diversification rates in mammals

We apply the birth-death diffusion model to the evolutionary history of mammals combining the latest time-calibrated species-level tree for the group (*36*) with their paleontological record. The dating of this tree is consistent with a more recent one with increased whole genome sampling (*10*) and supports a "long fuse" model of mammalian diversification with inter-ordinal divergences occurring mostly before, and intra-ordinal divergences after, the K-Pg boundary, particularly following the PETM (*37*). Applying the birth-death diffusion model to the species-level tree allows us to interpret node ages and branching patterns in terms of diversification dynamics.

We first estimated temporal variation of extinction rates from $84,576$ fossil occurrences using PyRate, a model that detects the number, magnitude and temporal placement of rate changes while controlling for sampling and preservation biases within a Bayesian framework (*30, 35*). We estimated such extinction curves independently for 14 major mammal clades, as well as for

Theria (placentals, marsupials and their extinct relatives) and Eutheria (placentals and their extinct relatives), used to constrain extinction rates for stem taxa (fig. S10). These curves recover a peak in extinction rates at the K-Pg (ca. 66 Mya) and PETM (ca. 55.5 Mya; fig. S10). The K-Pg caused high extinction of metatherians (marsupials and their extinct relatives) and stem eutherians; at the PETM, extinction targeted mostly stem eutherian lineages again, in concordance with previous evidence (*5*), and, to a lesser degree, Eulipotyphla. The completeness of the fossil record is very uneven across clades. More generally, the fossil record is subject to various sources of temporal, spatial and taxonomic preservation biases (*30*), which is reflected in different degrees of uncertainty around our extinction curve estimates (fig. S10). While these inherent biases affect any inference of deep-time dynamics, our measure of uncertainty around the extinction curves allows us to test the robustness of ours. In addition, in order to obtain per species extinction rate estimates we used clade-specific species-by-genus estimates, which are sensitive to current taxonomic knowledge. Different species-by-genus estimates would change the magnitude of the extinction curves but not their dynamics.

Applying our data augmentation inference of the birth-death diffusion model to the mammal phylogenetic tree, with extinction constrained by the fossil estimates, provided us with a posterior sample of complete mammal trees (Fig. 2A). Congruent with previous empirical assessments of diversification heterogeneity in mammals (*25*) and other groups (*23, 26, 38*), we find substantial variation across lineages in speciation rates (Fig. 2A,B), with a median posterior diffusion coefficient for speciation rates of $\sigma_\lambda = 0.063$, interpreted as an expected change of about 6.3% per My (Fig. 2C). Estimated lineage-specific speciation rates range from close to 0.005 events per lineage per My in some monotremes, up to more than 1.5 spp My^{-1} in Primatomorpha (Fig. 2A & fig. S11), with an average of about 0.7 spp My^{-1}. Primates experienced fast species turnover, characterized by both high speciation and extinction rates (fig. S11-S12). In comparison, the species rich rodents and bats have lower speciation rates, but were also less

affected by extinction, resulting in a faster accumulation of species than primates (Fig. 2A, fig. S11-S12). These results confirm the role played by differences in both speciation and extinction rates in explaining among-clade differences in present-day species richness (*33*). Over the full history of mammals, we estimate a posterior average of ca. $145,000$ extinct species (ca. 96% of species extinct). These estimates of past diversification and diversity are comparable to paleontological estimates (*33*).

At the scale of all mammals, we recover a clear mass extinction event at the K-Pg boundary (Fig. 3A). At the PETM, we find an almost imperceptible slow-down in species accumulation: the diversity loss experienced by mostly stem eutherians (fig. S10) is almost fully balanced by the radiation of crown placental lineages. We also applied the birth-death diffusion model using other extinction assumptions (no extinction, constant extinction, constant turnover, and extinction diffusion; figs. S14-17). Irrespective of the assumption on extinction, we consistently find an overall expectation for lineages to decrease their speciation rates by about 4% per My (posterior median for drift $\alpha = -0.044$, Fig. 2C). Analyses with extinction diffusion recover similar estimates of the diffusion coefficient for speciation rates to analyses with homogeneous extinction (figs. S14-S17), suggesting that the variability of speciation rates is not inflated when assuming homogeneous extinction. The analyses which did not use the fossil record to constrain extinction rates yielded lower diversity estimates, regardless of their respective extinction assumption (figs. S14-S17), and did not detect mass extinction events. This corroborates the importance of integrating fossil-based extinction rate estimates in recovering deep-time diversity dynamics (*33, 39*).

Extinction of slowly-speciating lineages at the K-Pg boundary

The average speciation rate across all therian mammals was relatively high and stable throughout the Jurassic, mirroring early crown mammal radiations (Fig. 3B) (*4*). This period was fol-

lowed by a decrease at the onset of the Cretaceous, and an increase during the late Cretaceous which led to the diversification of most extant placental orders (*10, 36*) (Fig. 3B,C). Coinciding with the K–Pg extinction event, average speciation rates increased abruptly (Fig. 3B,C). These temporal trends are robust to uncertainty around the phylogenetic tree and the extinction curves (fig. S13).

The abrupt increase of speciation rates at the K–Pg extinction event was driven by the extinction of slowly speciating lineages rather than a collective increase in speciation rates across lineages (Fig. 3D). Our results show that, on average, ca. 34% of therian diversity survived the K-Pg boundary (comparison at 67 and 65 Mya), with an average *pre*-K-Pg boundary speciation rate of ca. 0.78 spp My^{-1} for extinct lineages (predominantly stem metatherians and eutherians) and of ca. 0.88 spp My^{-1} for those that survived (Fig. 3D; mean difference of 0.096 spp My^{-1}, Welch's t-test $p < 10^{-99}$). This is driven mostly by the fact that metatherians, with slower speciation rates, experienced more extinctions than eutherians (average speciation rates at the outset of the K-Pg of 0.52 spp My^{-1} and 0.88 spp My^{-1}, with surviving percentages of 3.5% and 43%, respectively); indeed, only very few methaterians survived the K-Pg (posterior average of 4.25 lineages). The preferential extinction of slow speciating lineages also occurred both within metatherians and eutherians: it was particularly strong within metatherians (mean difference of 0.09 spp My^{-1}, Welch's t-test $p < 10^{-18}$), and marginally significant in eutherians (mean difference of 0.009 spp My^{-1}, Welch's t-test $p = 0.055$). This sorting process is expected under a model of 'speciational evolution' (i.e., speciation-driven phenotypic change), where clades undergoing frequent speciation have an evolutionary advantage (*40, 41*). At mass extinction events in particular, higher diversity and variability among descendant species increases the chances that at least one of them survives. These results differ from those expected under an 'explosive-rise' scenario of ecological release following mass extinctions and are not a necessary outcome of our model assumptions (fig. S18).

Of particular interest is whether mass extinctions primarily affected lineages with high background extinction rates. Although our (necessary) assumption of homogeneous extinction rates within each of the 16 clades precluded us from precisely evaluating this question at the species level, the fact that the K-Pg mass extinction event wiped out more metatherians, with lower background extinction rates (ca. 0.49 spp My^{-1} at the onset of the K-Pg boundary), than eutherians (0.61 spp My^{-1}) suggests this need not be the case (fig. S10). These results support a decoupling between background and mass extinctions (*42*). Regardless of the effect of background extinction rates, the disappearance of more slowly-speciating lineages at the K-Pg mass extinction event, rather than a collective increase of speciation rates across surviving lineages, resulted in an increase in average speciation rates (Fig. 3). After the K-Pg mass extinction event, speciation slowed-down (Fig. 3B). We found a decreasing trend across most of the Cenozoic, mirroring trends in rates of morphological evolution (*6*), until ca. early Miocene, where a surge in speciation rates is seen (Fig 3B,C; this pattern was also robust to phylogenetic uncertainty fig. S13), mostly driven by the renewed diversification of primates, artiodactyls and lagomorphs, and more recently, rodents (fig. S12).

Our results refute the explosive-rise and delayed-rise hypotheses wherein mammals were suppressed in their ecomorphological and taxonomic diversity during the Cretaceous and experienced a release at or after the K-Pg extinction event that spurred their diversification (*37*). Indeed, inference under simulations characterizing ecological release scenarios following (or not) mass extinction events do not conform to the empirical pattern observed across mammals (fig. S18). Instead, our results suggest an early-rise scenario, wherein rates of speciation increased before the K-Pg boundary, leading to the appearance of several major extant mammal orders (*3, 10*). Average speciation rates increased again at the K-Pg boundary, but because more slowly-speciating lineages were filtered out rather than it being due to an ecological release spurring diversification. This is concordant with recent phylogenetic and paleontological ev-

idence suggesting that a major ecomorphological and taxonomic diversification of mammals occurred before the K-Pg boundary coinciding with the rise of angiosperms (*4, 6, 43, 44*) and increased continental fragmentation (*10*). Underlying these overarching temporal patterns, however, we do not find a correlated burst of diversification across all mammals during the Late Cretaceous. Rather, early eutherian lineages alone drive this period of fast diversification (Fig. 3C). Presumably, this foregoing rise in diversification rates conferred several eutherian lineages higher probabilities to be represented by daughter lineages after the K-Pg boundary than, for instance, their metatherian counterparts.

These temporal trends were obtained by averaging over all lineages (observed and unobserved) in the complete trees thanks to our data augmentation approach, and would not have been properly characterized by only averaging over lineages that survived to the present and were sampled (figs. S11-S12).

Imbalanced speciation pulses

Under speciation dynamics driven by cross-lineage abiotic effects and infrequent evolutionary novelties (*12–16, 45*), we would expect a few scattered speciation rate shifts along the tree with subsequent homogeneous rates. Instead, we find substantial among-lineage heterogeneity, confirming recent results in birds (*26, 27*).

Bursts of speciation vary substantially in magnitude and seem to occur repeatedly, asynchronously and ephemerally. Indeed, dissecting among increases in speciation rates along the branches of the tree (or 'pulses'), we uncover a recurrent pattern of imbalanced, or asymmetrical, speciation rates, wherein, along consecutive nodes, only one of the daughter species sustains high speciation rate levels (Fig. 4). We characterized this imbalance for the largest pulses across mammals by quantifying the distribution of subsequent speciation rates (*30*). We found that the frequency of lineages with subsequent speciation rates that remain higher than the *pre*-pulse

speciation rate is usually around 50%, and never larger than 75% (fig. S19). This pattern holds across all our model assumptions on extinction (fig. S20-S23). In comparison, the same analyses performed on simulations with clade-level speciation shifts (*18, 20, 46*) result in $> 95\%$ of the speciation rates remaining higher than the *pre*-pulse level for the duration of the pulse (fig. S9). Such patterns of imbalanced speciation could arise from founder speciation events, frequently observed in speciation studies, in which small populations become isolated from the main population by chance events (*14, 47, 48*). Here, the initial low abundance of peripheral isolates limit their potential to generate new species, while the diversification potential of the main population remains largely unaffected (*14, 49*). This provides an interpretation for the observed tendency for speciation rates to decline through time (as evidenced by the negative estimate for α, Fig. 2C,4) due to imbalanced speciation rather than diversity-dependence (*50, 51*). This interpretation is further supported by the lack of evidence for speciation bursts at the aftermath of the K-Pg mass extinction, which would be expected if diversification was controlled by intra- or inter-clade diversity-dependent processes (fig. S18).

Conclusions

G. G. Simpson considered adaptive radiations, characterized by clade-wide shifts in speciation and diversity-dependent dynamics, to be the main source of life's extraordinary diversity (*13*). Our results support a more nuanced, dynamic and less predictable diversification process, wherein the complex interplay of species traits and the specific environment they experience periodically propitiate suitable conditions for separate speciation pulses. These ephemeral pulses reveal an imbalanced nature, in which a faster-speciating lineage gives rise to multiple slow-speciating ones. These, in turn, become increasingly vulnerable to extinction, often precipitated en masse during major environmental changes. While our findings underscore the role of contingency in diversification, general deterministic effects, including particular combinations

of body size (*52*) and dispersal propensity with certain landscape configurations (*10, 53, 54*), should increase the probability of occurrence and persistence of fast-speciating lineages. Diversity seems to depend on such lineages rather than on clade-wide adaptive radiations.

References

1. G. G. Simpson, *Tempo and mode in evolution*, no. 15 (Columbia University Press, 1944).
2. D. Schluter, *The ecology of adaptive radiation* (Oxford University Press, 2000).
3. R. W. Meredith, *et al.*, *Science* **334**, 521 (2011).
4. D. M. Grossnickle, S. M. Smith, G. P. Wilson, *Trends in Ecology & Evolution* **34**, 936 (2019).
5. N. S. Upham, J. A. Esselstyn, W. Jetz, *Current Biology* **31**, 4195 (2021).
6. A. Goswami, *et al.*, *Science* **378**, 377 (2022).
7. O. R. Bininda-Emonds, *et al.*, *Nature* **446**, 507 (2007).
8. T. Stadler, *Proceedings of the National Academy of Sciences* **108**, 6187 (2011).
9. M. S. Springer, N. M. Foley, P. L. Brady, J. Gatesy, W. J. Murphy, *Frontiers in Genetics* **10** (2019).
10. N. M. Foley, *et al.*, *Science* **380**, eabl8189 (2023).
11. E. Carlisle, C. M. Janis, D. Pisani, P. C. Donoghue, D. Silvestro, *Current Biology* **33**, 3073 (2023).
12. A. H. Miller, *Some ecologic and morphological considerations in the evolution of higher taxonomic categories* (Carl Winter, Heidelberg, Germany, 1949), p. 84–88.

13. G. G. Simpson, *The major features of evolution* (Columbia University Press, 1953).

14. E. Mayr, *Animal Species and Evolution* (Harvard University Press, 1963).

15. L. V. Valen, *Evolution* **25**, 420 (1971).

16. J. P. Hunter, *Trends in Ecology & Evolution* **13**, 31 (1998).

17. J. C. Willis, *Age and area; a study in geographical distribution and origin of species* (Cambridge [Eng.], The University press, 1922).

18. M. E. Alfaro, *et al.*, *Proceedings of the National Academy of Sciences* **106**, 13410 (2009).

19. R. S. Etienne, B. Haegeman, *The American Naturalist* **180**, E75 (2012).

20. D. L. Rabosky, *PloS one* **9**, e89543 (2014).

21. S. B. Heard, D. L. Hauser, *Historical biology* **10**, 151 (1995).

22. A. de Queiroz, *Systematic Biology* **51**, 917 (2002).

23. T. J. Davies, *et al.*, *Proceedings of the National Academy of Sciences* **101**, 1904 (2004).

24. M. J. Donoghue, *Paleobiology* **31**, 77 (2005).

25. T. J. Davies, *et al.*, *Proceedings of the National Academy of Sciences* **105**, 11556 (2008).

26. O. Maliet, F. Hartig, H. Morlon, *Nature ecology & evolution* **3**, 1086 (2019).

27. F. Ronquist, *et al.*, *Communications biology* **4**, 1 (2021).

28. S. J. Gould, *Is a New and General Theory of Evolution Emerging?* (Springer US, Boston, MA, 1987), pp. 113–130.

29. M. J. Benton, B. C. Emerson, *Palaeontology* **50**, 23 (2007).

30. Materials and methods are available as supplementary materials.

31. J. M. Beaulieu, B. C. O'Meara, *Evolution* **69**, 1036 (2015).

32. M. A. Tanner, W. H. Wong, *Journal of the American statistical Association* **82**, 528 (1987).

33. C. R. Marshall, *Nature Ecology & Evolution* **1**, 1 (2017).

34. D. Silvestro, R. Warnock, A. Gavryushkina, T. Stadler, *Nature Communications* **9**, 1 (2018).

35. D. Silvestro, N. Salamin, A. Antonelli, X. Meyer, *Paleobiology* **45**, 546–570 (2019).

36. S. Álvarez-Carretero, *et al.*, *Nature* **602**, 263 (2022).

37. J. D. Archibald, D. H. Deutschman, *Journal of Mammalian Evolution* **8**, 107 (2001).

38. S. B. Heard, *Evolution* **50**, 2141 (1996).

39. T. B. Quental, C. R. Marshall, *Trends in Ecology & Evolution* **25**, 434 (2010).

40. E. A. Lloyd, S. J. Gould, *Proceedings of the National Academy of Sciences* **90**, 595 (1993).

41. O. Sanisidro, M. C. Mihlbachler, J. L. Cantalapiedra, *Science* **380**, 616 (2023).

42. D. Jablonski, *Science* **231**, 129 (1986).

43. G. P. Wilson, *Through the End of the Cretaceous in the Type Locality of the Hell Creek Formation in Montana and Adjacent Areas* (Geological Society of America, 2014).

44. T. J. D. Halliday, A. Goswami, *Biological Journal of the Linnean Society* **118**, 152 (2016).

45. M. J. Benton, *Science* **323**, 728 (2009).

46. S. Höhna, *et al.*, *bioRxiv* (2019).

47. P. J. Wagner, D. H. Erwin, *Phylogenetic patterns as tests of speciation models* (Columbia University Press, New York, 1995), pp. 87–122.

48. B. T. Smith, *et al.*, *Nature* **515**, 406 (2014).

49. A. R. Templeton, *Genetics* **94**, 1011 (1980).

50. D. Moen, H. Morlon, *Trends in Ecology & Evolution* **29**, 190 (2014).

51. O. Hagen, K. Hartmann, M. Steel, T. Stadler, *Systematic Biology* **64**, 432 (2015).

52. M. Cardillo, *et al.*, *Science* **309**, 1239 (2005).

53. R. G. Moyle, C. E. Filardi, C. E. Smith, J. Diamond, *Proceedings of the National Academy of Sciences* **106**, 1863 (2009).

54. I. Quintero, M. J. Landis, W. Jetz, H. Morlon, *Proceedings of the National Academy of Sciences* **120**, e2220672120 (2023).

55. Data available in the Dryad data repository: DOI: 10.5061/dryad.5mkkwh7cs.

56. S. Nee, R. M. May, P. H. Harvey, *Philosophical Transactions of the Royal Society of London. Series B: Biological Sciences* **344**, 305 (1994).

57. C. Andrieu, G. O. Roberts, *The Annals of Statistics* **37**, 697 (2009).

58. O. Maliet, H. Morlon, *Systematic biology* (2021).

59. T. Stadler, *Systematic biology* **60**, 676 (2011).

60. R. G. FitzJohn, *Methods in Ecology and Evolution* **3**, 6 (2012).

61. R Core Team, *R: A Language and Environment for Statistical Computing*, R Foundation for Statistical Computing, Vienna, Austria (2022).

62. W. P. Maddison, P. E. Midford, S. P. Otto, *Systematic Biology* **56**, 701 (2007).

63. B. Horvilleur, N. Lartillot, *Bioinformatics* **30**, 3020 (2014).

64. I. Quintero, M. J. Landis, *Systematic Biology* **69**, 739 (2020).

65. N. G. Polson, G. O. Roberts, *Biometrika* **81**, 11 (1994).

66. T. Vasconcelos, B. C. O'Meara, J. M. Beaulieu, *bioRxiv* (2022).

67. J. Barido-Sottani, T. G. Vaughan, T. Stadler, *Systematic Biology* **69**, 973 (2020).

68. A. D. Barnosky, *Journal of Vertebrate Paleontology* **21**, 172 (2001).

69. J. Bezanson, A. Edelman, S. Karpinski, V. B. Shah, *SIAM Review* **59**, 65 (2017).

70. Mammal Diversity Database, Mammal diversity database (version 1.8) (2022).

71. D. L. Rabosky, *Evolution: International Journal of Organic Evolution* **64**, 1816 (2010).

72. S. Louca, M. W. Pennell, *Current Biology* **31**, 3168 (2021).

73. T. A. Heath, J. P. Huelsenbeck, T. Stadler, *Proceedings of the National Academy of Sciences* **111**, E2957 (2014).

74. D. Silvestro, J. Schnitzler, L. H. Liow, A. Antonelli, N. Salamin, *Systematic biology* **63**, 349 (2014).

75. M. Foote, *Paleobiology* **26**, 74 (2000).

76. J. Alroy, *Paleobiology* **40**, 374 (2014).

77. J. T. Flannery-Sutherland, N. B. Raja, Á. T. Kocsis, W. Kiessling, *Methods in Ecology and Evolution* **13**, 2404 (2022).

78. M. M. Pires, B. D. Rankin, D. Silvestro, T. B. Quental, *Biology letters* **14**, 20180458 (2018).

79. G. P. Wilson, *et al.*, *Nature* **483**, 457 (2012).

80. G. L. Benevento, R. B. Benson, R. A. Close, R. J. Butler, *Palaeontology* **66**, e12653 (2023).

81. D. M. Grossnickle, E. Newham, *Proceedings of the Royal Society B: Biological Sciences* **283**, 20160256 (2016).

82. C. V. Bennett, P. Upchurch, F. J. Goin, A. Goswami, *Paleobiology* **44**, 171 (2018).

83. G. P. Wilson, E. G. Ekdale, J. W. Hoganson, J. J. Calede, A. Vander Linden, *Nature communications* **7**, 13734 (2016).

84. J. L. Cantalapiedra, *et al.*, *Nature Ecology & Evolution* **5**, 1266 (2021).

85. J. L. Cantalapiedra, J. L. Prado, M. Hernández Fernández, M. T. Alberdi, *Science* **355**, 627 (2017).

86. J. L. Cantalapiedra, M. Hernandez Fernandez, B. Azanza, J. Morales, *Evolution* **69**, 2941 (2015).

87. M. Januario, T. B. Quental, *Evolution* **75**, 656 (2021).

88. C. J. Law, G. J. Slater, R. S. Mehta, *Systematic Biology* **67**, 127 (2018).

89. D. Silvestro, N. Salamin, J. Schnitzler, *Methods in Ecology and Evolution* **5**, 1126 (2014).

90. M. M. Pires, D. Silvestro, T. B. Quental, *Proceedings of the Royal Society B: Biological Sciences* **282**, 20151952 (2015).

366 91. M. M. Pires, D. Silvestro, T. B. Quental, *Evolution* **71**, 1855 (2017).

367 92. S. D. Tarquini, S. Ladevèze, F. J. Prevosti, *Scientific Reports* **12**, 1224 (2022).

368 93. C. Pimiento, *et al.*, *Nature ecology & evolution* **1**, 1100 (2017).

369 94. A. Solorzano, M. Nunez-Flores, *Palaeogeography, Palaeoclimatology, Palaeoecology*
370 **568**, 110306 (2021).

371 95. J. P. Herrera, *Evolution* **71**, 2845 (2017).

372 96. S. A. Fritz, *et al.*, *Proceedings of the National Academy of Sciences* **113**, 10908 (2016).

373 97. X. Lu, *et al.*, *Evolutionary Biology* **40**, 117 (2013).

374 98. M. Freudenthal, E. Martínez-Suárez, *Spanish Journal of Palaeontology* **28**, 239 (2020).

375 99. S. Renaud, *et al.*, *Proceedings of the Royal Society B: Biological Sciences* **272**, 609 (2005).

376 100. S. I. Quiñones, *et al.*, *Journal of South American Earth Sciences* **103**, 102701 (2020).

377 101. S. P. Zack, T. A. Penkrot, D. W. Krause, M. C. Maas, *Acta Palaeontologica Polonica* **50**,
378 809 (2005).

379 102. T. E. Williamson, A. Weil, *Acta Palaeontologica Polonica* **56**, 247 (2011).

380 103. S. P. Zack, *et al.*, *Papers in Palaeontology* **7**, 497 (2021).

381 104. J. John Sepkoski, *Philosophical Transactions of the Royal Society of London. Series B:*
382 *Biological Sciences* **353**, 315 (1998).

383 105. P. L. Forey, R. A. Fortey, P. Kenrick, A. B. Smith, *Philosophical Transactions of the Royal*
384 *Society of London. Series B: Biological Sciences* **359**, 639 (2004).

106. D. Jablonski, J. A. Finarelli, *Proceedings of the National Academy of Sciences* **106**, 8262 (2009).

107. P. L. Koch, A. D. Barnosky, *Annual Review of Ecology, Evolution, and Systematics* **37** (2006).

108. A. J. Stuart, *Geological Journal* **50**, 338 (2015).

109. D. Černỳ, D. Madzia, G. J. Slater, *Systematic Biology* **71**, 153 (2022).

110. M. Foote, D. M. Raup, *Paleobiology* **22**, 2 (1996).

111. I. Žliobaitė, M. Fortelius, *Paleobiology* **48**, 1 (2022).

112. K. Roy, D. Jablonski, J. W. Valentine, *Philosophical Transactions of the Royal Society of London. Series B: Biological Sciences* **351**, 1605 (1996).

113. J. D. Archibald, *Paleobiology* **19**, 1 (1993).

114. C. Patterson, A. B. Smith, *Nature* **330**, 248 (1987).

115. C. Patterson, A. B. Smith, *Ecology* **70**, 802 (1989).

116. L. J. Flynn, *et al.*, *Palaeogeography, Palaeoclimatology, Palaeoecology* **115**, 249 (1995).

117. N. S. Upham, J. A. Esselstyn, W. Jetz, *PLOS Biology* **17**, 1 (2019).

118. M. A. Suchard, *et al.*, *Virus evolution* **4**, vey016 (2018).

119. S. Louca, M. W. Pennell, *Nature* **580**, 502 (2020).

Acknowledgments

We thank Juan L. Cantalapiedra and Juan D. Carrillo for advice in compiling fossil information and Daniele Silvestro for advice in running the PyRate analyses. We thank Joëlle Barido-Sottani, the Morlon lab in general, Nathan Upham and two other anonymous referees for comments on the manuscript. **Funding:** This project has received funding from the European Union's Horizon 2020 research and innovation programme under the Marie Skłodowska-Curie grant agreement No. 897225 for IQ. HM acknowledges funding from the European Union's Horizon 2020 research and innovation programme under the ERC CoG PANDA, and from the French National Research Agency under the ANR CHANGE. **Author contributions:** I.Q. and H.M. designed the study; I.Q. derived, developed and implemented the model and code and carried out the empirical application; N.L. contributed to the data augmentation algorithm; and I.Q. and H.M. wrote the paper; I.Q., N.L., and H.M. edited the manuscript. **Competing interests:** The authors declare no competing interests. **Data and materials availability:** Software to run all models is available in the Tapestree.jl package (https://github.com/ignacioq/Tapestree.jl). All other code and data is available in the Dryad data repository: DOI: 10.5061/dryad.5mkkwh7cs.

Supplementary materials

Materials and Methods

Figs. S1 to S23

References (56–119)

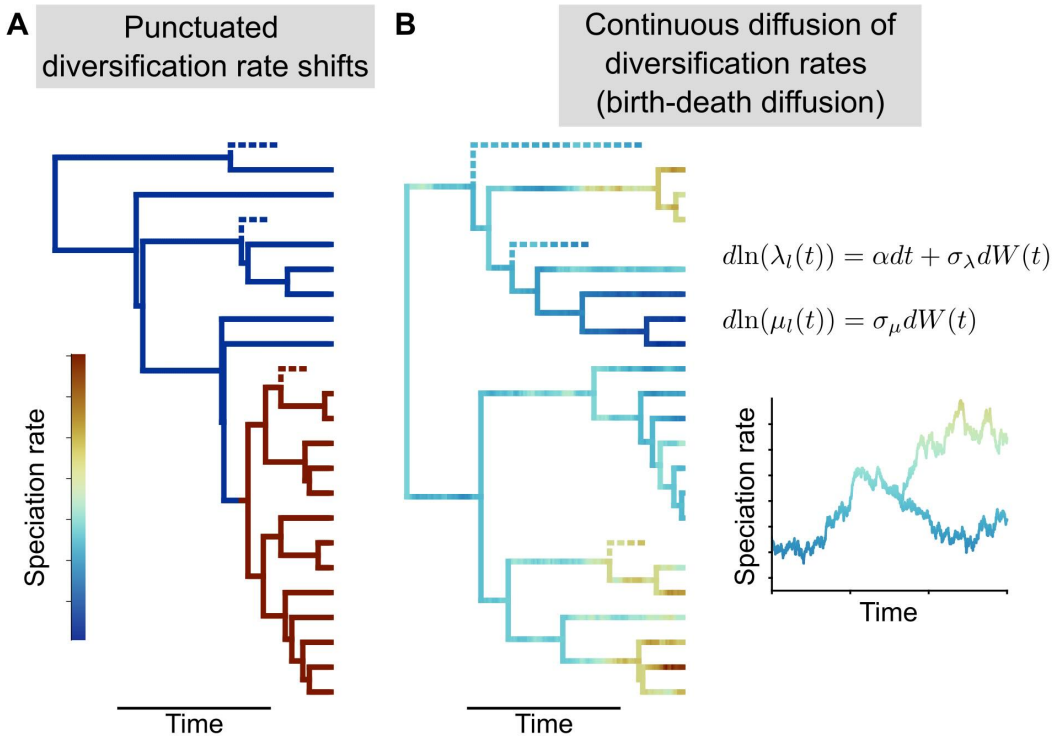

Fig. 1: Punctuated versus diffused changes in diversification. Hypothetical evolutionary history of a clade under two contrasting views of diversification, highlighted by differences in how speciation rates vary: **(A)** Punctuated shifts in speciation, here shown as a clade-wide discrete increase (red) from the background rate (blue) as predicted by, for example, the sudden appearance of adaptive innovations. **(B)** Diffusion of speciation rates, assumed under our birth-death diffusion model, as predicted by a temporally dynamic interplay between species traits and their environment. In the birth-death diffusion model, for lineage l at time t, the changes in speciation $\lambda_l(t)$ and extinction $\mu_l(t)$ rates during a small time dt are given by the Geometric Brownian process, which equations are shown in the figure. Here α represents a drift term, σ_λ and σ_μ the diffusion rates, and $W(t)$ is the Wiener process (i.e., standard Brownian motion). Lineages that are not observed in the phylogenetic tree of present-day species because they went extinct are represented with dashes. Our data augmentation framework takes a tree of present-day species as input and outputs posterior samples of complete trees, including both observed and unobserved lineages, with associated rate estimates.

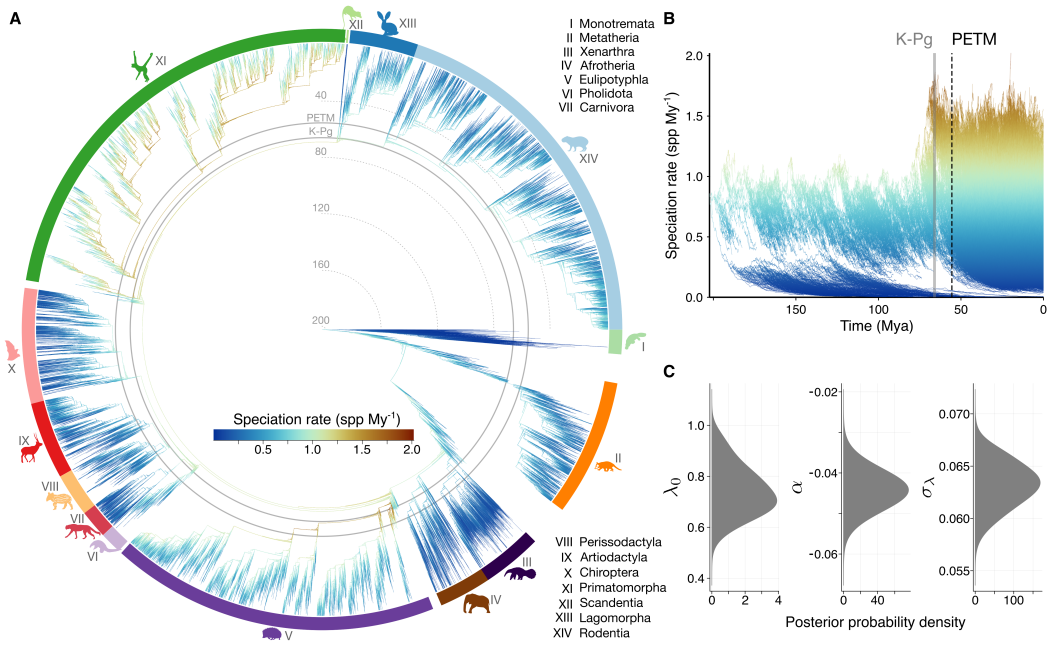

Fig. 2: Mammal diversification dynamics informed by their phylogeny and fossils, under the birth-death diffusion model with extinction rates estimated from the fossil record. **(A)** Complete radiation of mammals, incorporating the tree of extant species and lineages that went extinct or were not sampled at present (one representative complete tree sample from the birth-death diffusion posterior); warmer colors represent higher speciation rates. Surrounding colored radian arcs identify the crown plus stem diversity of the 14 mammal clades with embedded species silhouettes from PhyloPic (phylopic.org) and roman numerals for identification. Lineages without any surrounding color correspond to those that are not part of the stem diversity of any of these clades (e.g., stem therians and eutherians). Radial dashed gray lines specify the timescale every 40 My into the past, and solid circular grey lines specify, in order, the Cretaceous-Paleogene mass extinction event (K-Pg) and Paleocene-Ecocene Thermal Maximum (PETM). **(B)** Lineage speciation rates through time plotted for the same complete tree sample as in A. The grey solid line demarcates the K-Pg boundary and the black dashed line the PETM. **(C)** Posterior distributions for the three parameters of the birth-death diffusion model (with extinction estimated from the fossil record): speciation rate at the root λ_0, drift α, and diffusion in speciation rates σ_λ.

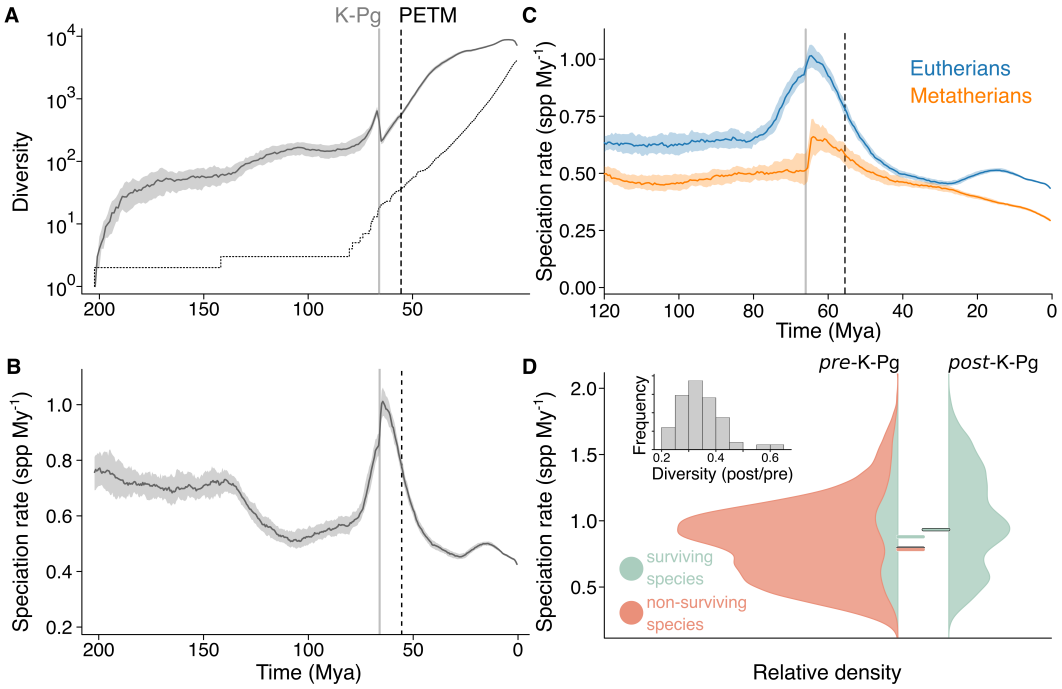

Fig. 3: Wiping out of slow-speciating lineages during the K-Pg mass extinction event. **(A)** Distribution through time of the estimated number of therian mammal lineages (placentals, marsupials and their extinct relatives; solid line shows the median, shade the 50% Credible Interval 'CI'). Dotted line shows the Lineage-Through-Time plot obtained from the tree of present-day mammals. **(B)** Average speciation rates across all therian mammals, displaying an increase before the K-Pg, followed by a sharp increase at the K-Pg boundary, with slowdown in the aftermath. Solid line shows the median and shade the 50% CI, across all data augmented trees. **(C)** Average speciation rates (median and 50 % CI across all data augmented trees) for eutherians (placentals and their extinct relatives, in blue) and metatherians (marsupials and their extinct relatives, in orange). Speciation rates increased before the K-Pg boundary in eutherians, but not metatherians. They then increased abruptly at the K-Pg boundary in metatherians and, to a lesser extent, in eutherians. **(D)** Density distributions of speciation rates before the onset (67 Mya) and end (65 Mya) of the K-Pg boundary across all data augmented trees, colored by lineages that survived (light blue) or went extinct (pink). Horizontal lines show the average speciation rates for each of these groups, colored respectively, and combined (black). Inset shows the posterior frequency distribution of the proportion of therian mammal diversity that survived the K-Pg extinction event, across all data augmented trees.

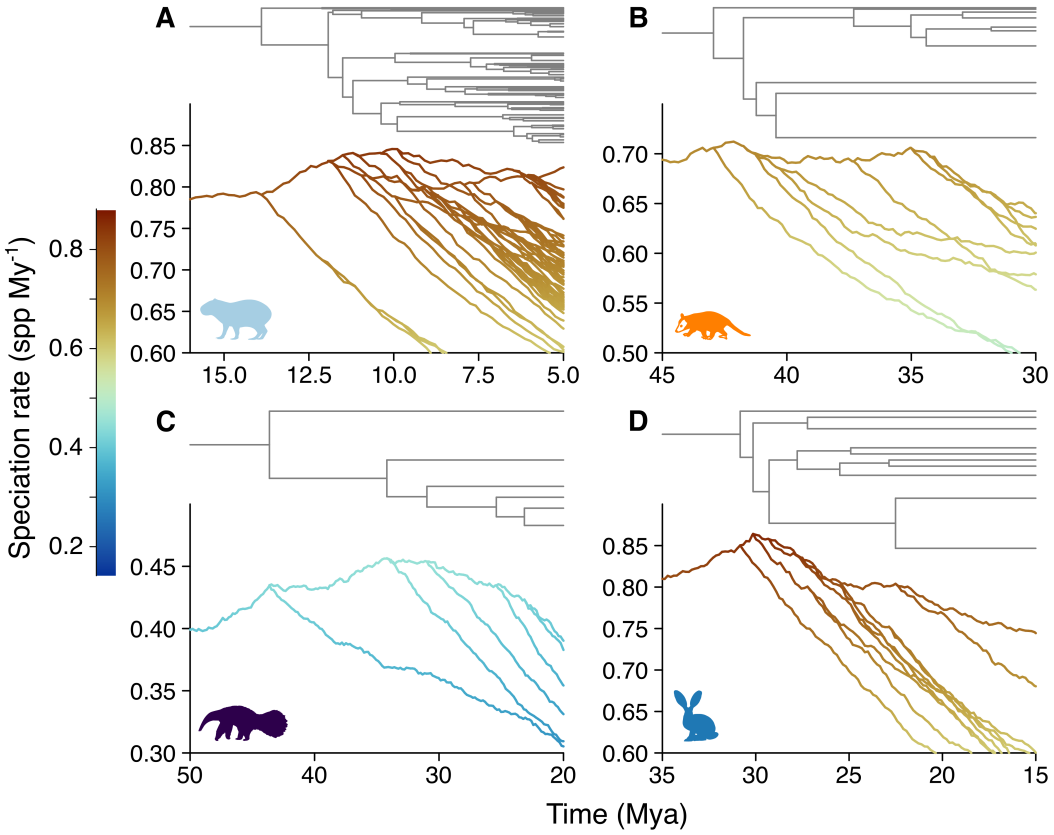

Fig. 4: Imbalanced speciation in mammals. Four illustrative examples of how speciation rates vary in the mammal tree, obtained by zooming into parts of the tree of: **(A)** Rodentia **(B)** Marsupialia **(C)** Xenarthra, and **(D)** Lagomorpha. For each panel we show at the top, in gray, the section of tree, and at the bottom, the evolution of speciation rates along the respective branches, represented both by color and the position on the y axis. For clarity, we show posterior median lineage-specific speciation rates in the tree of present-day mammals, rather than complete trees with extinct lineages.